Numerical extraction of Rayleigh waves and assessment of their influence on liquefaction damage

Extraction numérique des ondes de Rayleigh et évaluation de leur influence sur les dégâts de liquefaction

Kentaro Nakai
Department of Civil Engineering, Nagoya University, Japan, nakai@civil.nagoya-u.ac.jp

Akira Asaoka
Association for the Development of Earthquake Prediction, Japan

ABSTRACT: One of the important characteristics of surface waves is that distance attenuation is small compared with body waves. However, the influence of surface waves on liquefaction damage has not been fully understood yet. This paper tries to extract the surface waves (Rayleigh waves) and assess their influence on liquefaction damage with the use of 2D elasto-plastic effective stress analysis considering the effect of irregularly shaped bedrock. As a result, the importance of multidimensional effects such as the propagation of surface waves was emphasized for accurate and reasonable liquefaction damage prediction. The new findings are as follows: 1) Due to the propagation of Rayleigh waves, the risk of liquefaction calculated from 2D analysis becomes higher compared with 1D analysis. 2) Localized and extensive liquefaction damage was produced by the complex interference between the Rayleigh waves and body waves, which is known as the "edge effect." 3) The influence of Rayleigh waves on liquefaction damage is significantly large even when the acceleration level of Rayleigh waves is quite small.

RÉSUMÉ : Une caractéristique importante des ondes de surface est que leur atténuation par la distance est faible par rapport aux ondes transversales. Cependant, l'influence des ondes de surface sur les dégâts de liquéfaction n'est pas encore complètement comprise. Cet article tente d'extraire les ondes de surface (ondes de Rayleigh) et d'évaluer leur influence sur les dégâts de liquéfaction au moyen d'une analyse 2D élasto-plastique des contraintes effectives en tenant compte des effets d'un substrat rocheux de forme irrégulière. Par conséquent, l'importance des effets multi-dimensionnels, tels que la propagation des ondes de surface, a été soulignée pour obtenir une prédiction précise et raisonnable des dégâts de liquéfaction. Les nouvelles découvertes sont les suivantes: 1) En raison de la propagation des ondes de Rayleigh, le risque de liquéfaction calculé à partir de l'analyse 2D est supérieur à celui de l'analyse 1D. 2) des dégâts de liquéfaction localisés et importants ont été causés par les interférences complexes entre les ondes de Rayleigh et les ondes transversales, ce qui est connu sous le nom "effet de bord". 3) L'influence des ondes de Rayleigh sur les dégâts de liquéfaction est significativement importante, même quand leur niveau d'accélération est assez faible.

KEYWORDS: Rayleigh waves, irregularly shaped bedrock, liquefaction

1 INTRODUCTION

In December 2015, the Cabinet Office published its "Report on Long Period Seismic Motions due to a Major Earthquake along the Nankai Trough". Long period seismic motions are seismic motions with somewhat long periods in the order of 2 to 10 seconds, and they are of concern due to an increase in seismic damage resulting from resonance, such as in the case of large oscillations of ultra high-rise buildings over a long duration or sloshing of gasoline tanks. The main component of these long period seismic motions are said to be surface waves produced at irregularly shaped boundaries between hard bedrock near the surface and soft deposited strata. One of the important characteristics of surface waves is that distance attenuation is small during propagation, so they can be transmitted several hundred kilometers from the epicenter.

In the Hyogo-ken Nanbu Earthquake (1995), damage to housing was concentrated in a narrow area at the foot of the Southern Rokko Mountains that is distant from the epicenter fault. The cause of the localization of the seismic damage into so-called "seismic damage bands" is the "edge effect (Kawase and Matsushima 1998)", as shown in Fig. 1. As a result of the underground geological structure, in which the bedrock dips greatly from the Rokko Mountains toward Osaka Bay, a horizontally transmitted surface wave generated at the edge of the rock at the mountain side interferes with and is amplified by a body wave passing through the deposited strata at a specific position on the surface.

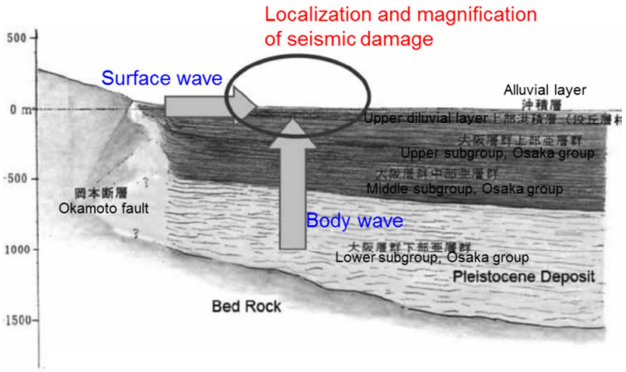

Figure 1 Band of seismic damage produced by interference of surface waves and body waves at the edge of bedrock

By studying seismic damage from the past, many similar examples of increase and localization of oscillations and liquefaction damage caused in this type of irregularly shaped ground have been found. However, it is difficult to extract surface waves only from actual seismic records, so the effect of surface waves on the oscillations of surface strata is not sufficiently understood. Also, in the damage predictions for a major earthquake (maximum class) in the Nankai Trough published by the Cabinet Office in August 2012, it is envisaged that there will be strong oscillations and a high probability of

liquefaction in the Pacific alluvial plain and in reclaimed ground. Although these predictions were made on the basis of equivalent linear analysis or nonlinear analysis (total stress analysis) based on G-γ and h-γ curves, they were just vertical 1-dimensional analyses. Moreover, in the seismic response analyses normally carried out, the assumption of horizontally stratified ground is frequently made to simplify the ground model. Therefore, these analyses do not take into consideration multidimensional effects such as the generation of surface waves due to irregular soil stratification and bedrock structure, so there is a danger that the oscillations on the ground surface and the liquefaction hazard will be underestimated.

In this paper, 2-dimensional elasto-plastic effective stress analysis is carried out taking into consideration irregularity of the ground stratification, Rayleigh waves are numerically reproduced and extracted from among the surface waves generated from the irregular bedrock, and the effect on the liquefaction hazard of the surface strata is investigated. The analysis code used was *GEOASIA* (Noda, T. et al 2008), a soil-water coupled finite deformation analysis code that incorporates an elasto-plastic constitutive model (the SYS Cam-clay model (Asaoka, A. et al 2002)) that describes soils including sand, intermediate soils, and clays in the same theoretical framework.

2 ANALYSIS CONDITIONS

The analysis model is shown in Fig. 2. A ground model with a height of 100 m and length of 30,000 m was produced. The stratification composition consisted of (from the bottom) hard bedrock, soft alluvial clay, and alluvial sand with a high potential for liquefaction. A slope was provided at the boundary between the clay stratum and bedrock in the part 2,700 m from the left end, with reference to the Urayasu soil composition. In the example in this paper, the slope angle was 3°. The elasto-plastic properties used in the analysis are shown in Table 1. All the parameters were determined from the insitu surveys and laboratory tests using undisturbed specimen at Urayasu. The details are shown in Nakai, K. et al 2015. The hydraulic boundaries were set so that the water level surface coincided with the ground surface and the water pressure at the ground surface was always zero, and the bottom end and the two side surfaces were undrained.

Input seismic motion is shown in Fig. 3. This was from the Off the Pacific Coast of Tohoku Earthquake which had a long duration and various period bands ranging from short periods to long periods. The EW component of the seismic wave measured at GL-36 m at the Tokyo Metropolitan Government Bureau of Port and Harbor Shinagawa Seismological Observatory. The above seismic motion was considered to be 2E waves and were uniformly input over the excitation area shown in Fig. 2 in the horizontal direction. During the earthquake, the boundaries at both side ends were set as lateral boundary element simple shear deformation boundaries, and in order to prevent the reflection of waves at the right end, in a region about 1,000 m from the end, the derivative of the acceleration with respect to time, the acceleration, and the velocity values were forcibly set to zero every 1 second. Also, all the nodes on the bottom surface of the ground including the excitation region employed a viscous boundary equivalent to V_s = 400 m/s.

Table 1 Material constants and initial conditions used for the analysis

		Sand	Clay	Bedrock
Elasto-plastic parameters	NCL intercept N	2.00	3.02	2.00
	Critical state index M	1.40	1.40	1.50
	Compression index $\tilde{\lambda}$	0.10	0.242	0.005
	Swelling index $\tilde{\kappa}$	0.0025	0.02	0.0005
	Poasson's ratio ν	0.2	0.1	0.1
Evolution parameters	Ratio of $-D_v^p \,\&\, \|D_s^p\|$ c_s	1.0	0.4	0.5
	Degradation index of STR $a(b=c=1.0)$	8.0	0.65	0.05
	Degradation index of OCR m	8.0	20.0	0.3
	Rotational hardening index br	10.0	0.2	0.2
	Limitation of rotational hardening m_b	0.44	1.0	0.7
Physical properties	Soil particle density ρ_s (g/cm^3)	2.787	2.69	2.65
	Mass permeability index k (cm/s)	1.0×10^{-4}	10×10^{-7}	$1.\times10^{-6}$
Initial conditions	Specific volume v_0	1.98	3.35	1.21
	Stress ratio η_0	0.545	0.545	0.545
	Degree of STR $1/R^*_0$	3.04	21.75	100
	Degree of anisotropy ς_0	0.545	0.545	0.545
	Degree of OCR $1/R_0$	Distributed in accordance with overburden pressure		

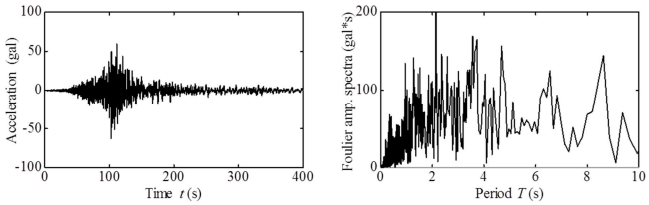

Figure 3 Input seismic motion

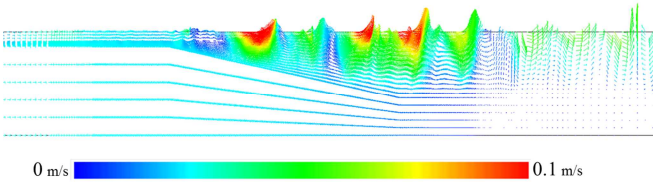

Figure 4 Generation of Rayleigh waves at the sloping base end

3 NUMERICAL EXTRACTION OF RAYLEIGH WAVES

Figure 4 shows the velocity vector distribution near the sloping part of the bedrock 150 seconds after occurrence of the earthquake. It can be seen that surface waves (Rayleigh waves)

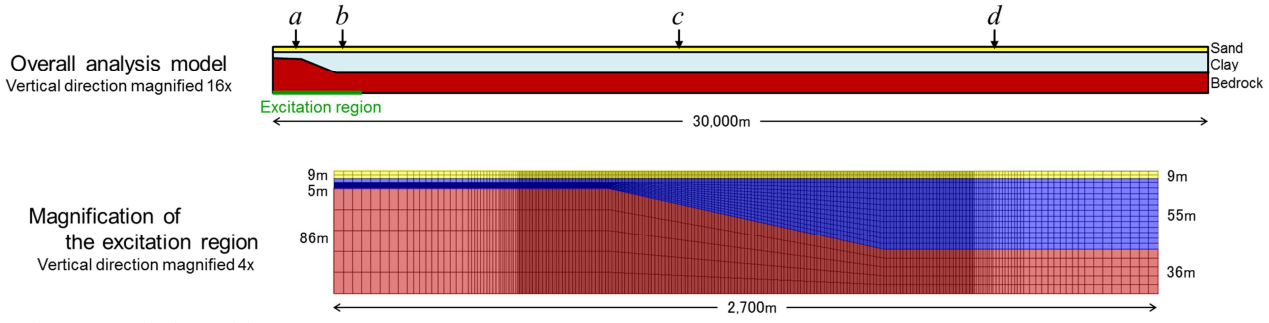

Figure 2 Analysis model

are generated in the surface stratum, heaving up in the counterclockwise direction. These Rayleigh waves are generated at the sloping bedrock and proceed to the right in the figure. Figures 5 to 8 show the acceleration properties of the surface waves at points *a* to *d* in Fig. 1. Comparing points *a* and *b* directly above the excitation region, there is no big difference in the maximum acceleration in the horizontal direction. However, at point *a*, short period components of 1 second or less predominate, and in contrast, at point *b*, there is significant acceleration amplification in the period band at around 2 seconds associated with passage through the thickly deposited clay stratum. Also, as a result of the effect of Rayleigh waves, it can be seen that at point *b*, comparatively strong oscillations are generated that continue for more than 200 seconds after the end of the main motion, the "post-motion phenomenon," and that movement is generated in the vertical direction, although the seismic input was in the horizontal direction only. Also, looking at points *c* and *d*, which are 10,000 m and 20,000 m from the excitation region, it can be seen that accelerations of a maximum of 20 gal are propagated in both the horizontal and vertical directions. At both points, there is no acceleration response at the bottom end, so there is virtually no effect from body waves. It is therefore considered that the waves extracted in Figs. 7 and 8 are simple Rayleigh waveforms.

4 EFFECT OF RAYLEIGH WAVES ON LIQUEFACTION

Figure 9 shows the shear strain distribution at 100, 200, and 800 seconds after the start of the seismic motion input. Between 100 seconds and 200 seconds, the region of occurrence of shear strain spreads to the right, and the pattern of propagation of Rayleigh waves can be seen. Focusing on the area around the excitation region at 800 seconds after a certain amount of time has passed since the end of the seismic input, even though the sandy soil of the surface stratum was assumed to be uniform, the pattern of occurrence of shear strain was planarly nonuniform, and in particular, in the region to the right of the sloping part, the shear strain was locally increased. This is due to the edge effect, in which the body waves from deep below

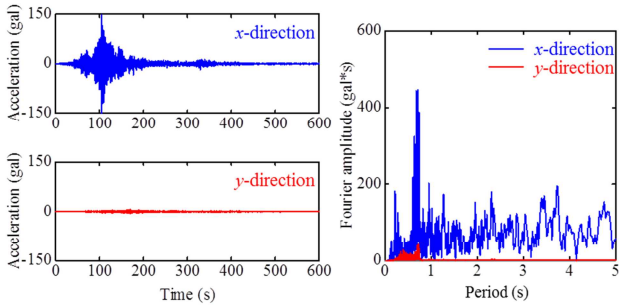

(a) Acceleration response in the *x* and *y* directions on the ground surface (b) Fourier amplitude spectrum of the ground surface response

Figure 5 Acceleration properties of the surface waves at point *a* (effect of body waves)

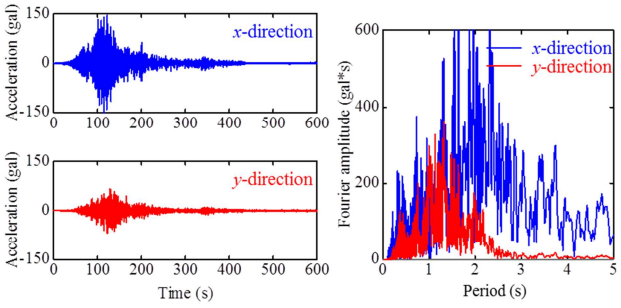

(a) Acceleration response in the *x* and *y* directions on the ground surface (b) Fourier amplitude spectrum of the ground surface response

Figure 6 Acceleration properties of the surface waves at point *b* (effect of body waves + Rayleigh waves)

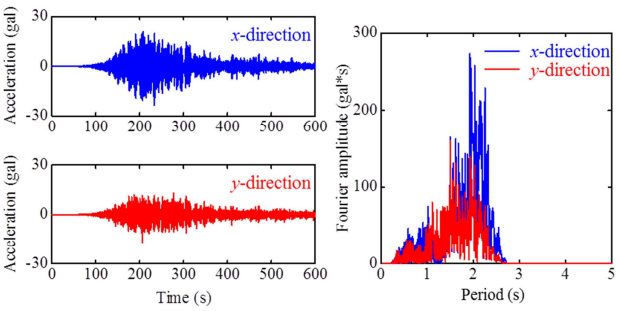

(a) Acceleration response in the *x* and *y* directions on the ground surface (b) Fourier amplitude spectrum of the ground surface response

Figure 7 Acceleration properties of the surface waves at point *c* (effect of Rayleigh waves)

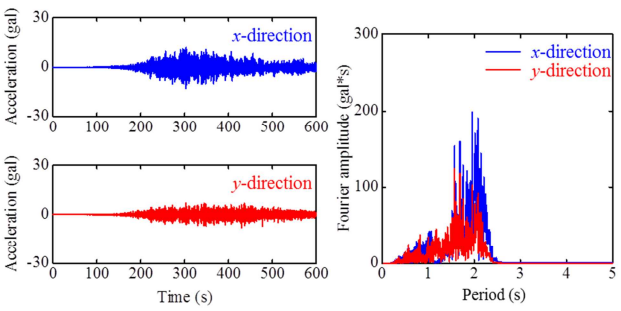

(a) Acceleration response in the *x* and *y* directions on the ground surface (b) Fourier amplitude spectrum of the ground surface response

Figure 8 Acceleration properties of the surface waves at point *d* (effect of Rayleigh waves)

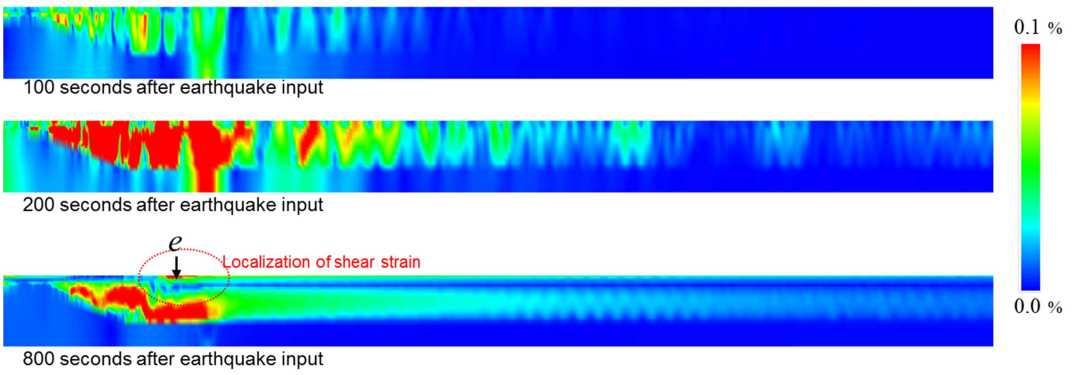

Figure 9 Rayleigh wave propagation and damage localization as seen from the distribution of shear strain

and the Rayleigh waves propagated along the surface interfere in specific regions, as shown in Fig. 1.

A new point, *e*, where the shear strain was localized, was newly defined, and the effect on liquefaction damage was investigated. The mean effective stress reduction ratio in the surface stratum sandy soil is shown in Fig. 10 for point *a* on the left of the excitation region, in Fig. 11 for points *b* and *e* to the right of the excitation region, and in Fig. 12 for points *c* and *d* at a distance from the excitation region.

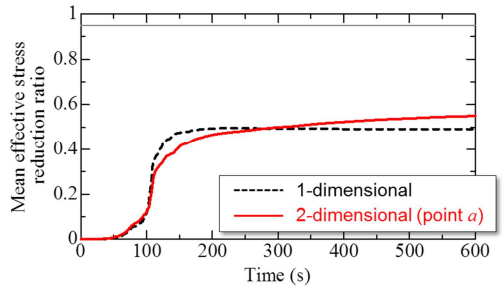

Figure 10 Reduction ratio at point *a* on the left of the excitation region

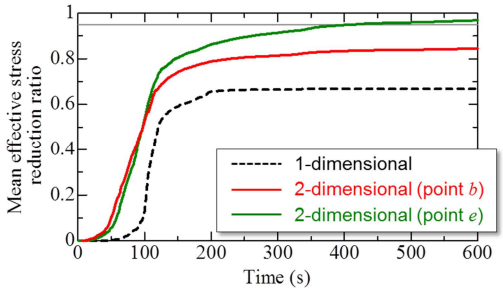

Figure 11 Reduction ratio at points *b* and *e* on the right of the excitation region

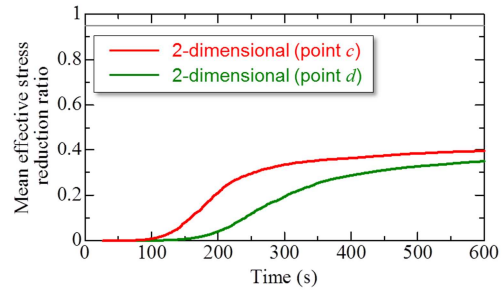

Figure 12 Reduction ratio at points *c* and *d*, distant from the excitation region (effect of Rayleigh waves)

In Figs. 10 and 11, 1-dimensional analysis results for the same stratigraphic composition as points *a*, *b*, and *e* are also shown in order to determine the 2-dimensional effect (Rayleigh waves). From the 1-dimensional analysis results, it can be seen that the mean effective stress reduction ratio increases rapidly from near the main motions (from the start of the earthquake to about 100 seconds), but from 200 seconds onwards, when the seismic motion is complete, steady state conditions are reached, and there is no liquefaction at any of points *a* (Fig. 10) *b* (Fig. 11) or *e* (Fig. 11). The mean effective stress reduction ratio is greater at points *b* and *e*, where the clay stratum is thick, than at point *a*, but as stated previously, this is because the long period components are amplified in the clay stratum, so a large shear deformation is produced even if there is no difference in the maximum acceleration. Comparing the 1-dimensional analysis and the 2-dimensional analysis, it can be seen that there is no major difference between the two at point *a* (Fig. 10) located on the left side of the sloping base end, where the effect of Rayleigh waves is small. However, at points *b* and *e* (Fig. 11), which are affected by Rayleigh wave propagation, the increase in the mean effective stress reduction ratio is earlier in the 2-dimensional analysis, and the amount of reduction is also larger. At point *b*, the liquefaction state (95% or higher) is not reached, but at point *e*, where the shear strain is localized, the mean effective stress reduction ratio continues to gently increase from 200 seconds onwards after the main seismic motion has stopped and ultimately exceeds 95% where liquefaction occurs. Points *b* and *e* are the same model in the 1-dimensional analysis, but when multidimensional effects such as Rayleigh waves and refraction/reflection of waves at the slope are taken into consideration, the extent of damage is different, and it can be seen that the liquefaction hazard is greater than that indicated by the 1-dimensional analysis. Finally, at points *c* and *d*, where only Rayleigh waves were propagated (Fig. 12), the mean effective stress reduction ratio gradually increased to 40%, even though the maximum acceleration was small at about 20 gal. Although liquefaction did not occur at both points, the Rayleigh waves included quite long period components, so the liquefaction hazard was increased. Note that at the distant point d, there was a gentle increase with time, but this was caused by the dispersibility of the Rayleigh waves.

5 CONCLUSIONS

In this paper, 2-dimensional elasto-plastic effective stress analysis was carried out taking into consideration irregularity of the ground stratification, Rayleigh waves were numerically reproduced and extracted from among the surface waves generated from the irregular bedrock, and the effect on the liquefaction hazard of the surface strata was investigated. The results showed that (1) as a result of the effect of the Rayleigh waves, the liquefaction hazard was higher in the 2-dimensional analysis than in the 1-dimensional analysis; (2) there are places where the liquefaction damage was increased locally due to interference between Rayleigh waves and body waves, and (3) the mean effective stress reduction ratio was greatly increased even with only Rayleigh waves, so Rayleigh waves greatly affect the liquefaction hazard.

Most of the existing damage prediction methods not only do not substantially take into consideration the nonlinearity of the ground but also are vertical 1-dimensional evaluations, so multidimensional effects due to an irregular stratigraphic and bedrock structure are not taken into consideration. The analysis results in this paper indicate that multidimensional effects as represented by the generation and propagation of Rayleigh waves are not so small that they can be ignored and are an item that should be considered for more precise damage predictions that conform with the actual situation.

6 REFERENCES

Cabinet Office. 2015. Report on Long Period Seismic Motions due to a Major Earthquake along the Nankai Trough.

Kawase, H. and Matsushima, S. 1998. Three-dimensional Wave Propagation Analysis of Simple Two-dimensional Basin Structures with Special Reference to "the Basin-Edge Effect", Jishin, Vol. 50 (4), pp. 431-449.

Cabinet Office. 2013. Damage Predictions for a Major Earthquake in the Nankai Trough (Second Stage Report).

Noda, T., Asaoka, A. and Nakano, M. 2008. Soil-water coupled finite deformation analysis based on a rate-type equation of motion incorporating the SYS Cam-clay model, S&F, 48(6), 771-790.

Asaoka, A., Noda, T., Yamda, E., Kaneda, K. and Nakano, M. 2002. An elasto-plastic description of two distinct volume change mechanisms of soils, S&F, 42(5), 47-57.

Nakai, K., Asaoka, A. and Sawada, Y. 2015. Liquefaction damage enhanced by interference between body waves and induced surface wave on inclined bedrock, JGS Special Pub. 2(19), 723-728.